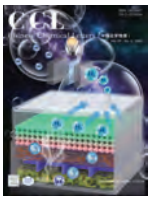
Chinese Chemical Letters 37 (2026) 111892

Contents lists available at ScienceDirect

Chinese Chemical Letters

journal homepage: www.elsevier.com/locate/cclet



Electrochemical strategies for advancing enantioselective enamine catalysis

Dengke Ma[a,*], Youai Qiu[b,*]

[a] School of Pharmaceutical Sciences, Capital Medical University, Beijing 100069, China
[b] State Key Laboratory and Institute of Elemento-Organic Chemistry, Frontiers Science Center for New Organic Matter, Haihe Laboratory of Sustainable Chemical Transformations, College of Chemistry, Nankai University, Tianjin 300071, China

ARTICLE INFO

Article history:
Received 25 June 2025
Revised 3 September 2025
Accepted 24 September 2025
Available online 24 September 2025

Keywords:
Electrochemistry
Asymmetric catalysis and synthesis
Enamine catalysis
Stereocontrol
Radical chemistry

ABSTRACT

Enantioselective enamine catalysis has enriched asymmetric synthesis by enabling precise stereochemical control. While classically thermal/photochemical strategies have expanded reaction diversity, electrochemical enantiocontrol remains underexplored despite its potential for tunable redox manipulation. This review systematically evaluates electrochemical enantioselective enamine catalysis through polar/radical mediated chemical bond formation pathways, aiming to delineate current mechanistic paradigms and highlight electrochemistry's unique role on asymmetric enamine catalysis beyond thermodynamic and photochemical conditions. Future efforts including developing enhanced compatibility of chiral catalysts and intermediates with electrochemical systems, as well as exploiting transformative techniques for mechanistic elucidation could be promising to unlock more novel transformations and stereoselectivity models.

© 2026 Published by Elsevier B.V. on behalf of Chinese Chemical Society and Institute of Materia Medica, Chinese Academy of Medical Sciences.

1. Introduction

The enantioselective synthesis of functionalized carbonyl compounds continues to represent a fundamental research priority across chemical sciences, with particular significance in synthetic methodology development and pharmaceutical manufacturing [1–4]. Within this context, enamine catalysis has emerged as a pivotal strategy, deriving its value from a synergistic combination of stereochemical precision, operational efficiency, and sustainable practice. The classical paradigm of enantioselective enamine catalysis involves stereodefined bond formation (C–C/C-X) through nucleophilic engagement of chiral enamine intermediates with electrophilic partners, effectively establishing α-stereocenters in carbonyl frameworks [4–16]. This polar chemical bond formation mechanism (Fig. 1A-i) operates through directed electron pair transfer from the electron-rich enamine species to the electrophilic counterpart, enabling predictable stereochemical outcomes.

In continuous developments, the strategic implementation of radical mediated chemical bond construction *via* radical species has expanded the synthetic utility of enamine systems. Current mechanistic frameworks can be predominantly classified into two distinct categories based on enamine intermediate forms: (i) Stereocontrolled coupling of SOMO-philes with chiral enamine radical cations generated through single-electron oxidation (Fig. 1B-i) [17–19]. (ii) Stereoselective interception of electrophilic radicals by ground state enamine species [19,20], triggered by single electron reduction from excited photocatalysts [19,21–25], photoexcitation of chiral EDA complex including chiral enamine [26], direct photoexcitation of chiral enamine to be a strong single electron reductant (Fig. 1B-ii) [27–29].

Recent years, synthetic electrochemistry has undergone significant growth. By harnessing electrical energy as a traceless redox equivalent, this approach fundamentally circumvents the reliance on stoichiometric chemical oxidants or reductants for traditional thermodynamic reactions, thereby aligning with green chemistry principles. This paradigm shift not only enhances synthetic efficiency but also expands the chemical space accessible for precision molecular editing and functional group manipulation [30–44]. Within enantioselective enamine catalysis, its combination with electrochemistry also brings many innovative transformations in line with the goal of acquisition optical α-stereocentered carbonyl compounds in a more efficient, economic, and greener manner.

So far, electrochemical enamine catalysis has seen its success in above mentioned polar and radical mediated transformations. For instance, electrochemical oxidation converts substrates to active electrophiles *via* multi-electron transfer; these species then react with chiral enamines through polar pathways to deliver products

* Corresponding authors.
E-mail addresses: madk@ccmu.edu.cn (D. Ma), qiuyouai@nankai.edu.cn (Y. Qiu).

https://doi.org/10.1016/j.cclet.2025.111892
1001-8417/© 2026 Published by Elsevier B.V. on behalf of Chinese Chemical Society and Institute of Materia Medica, Chinese Academy of Medical Sciences.

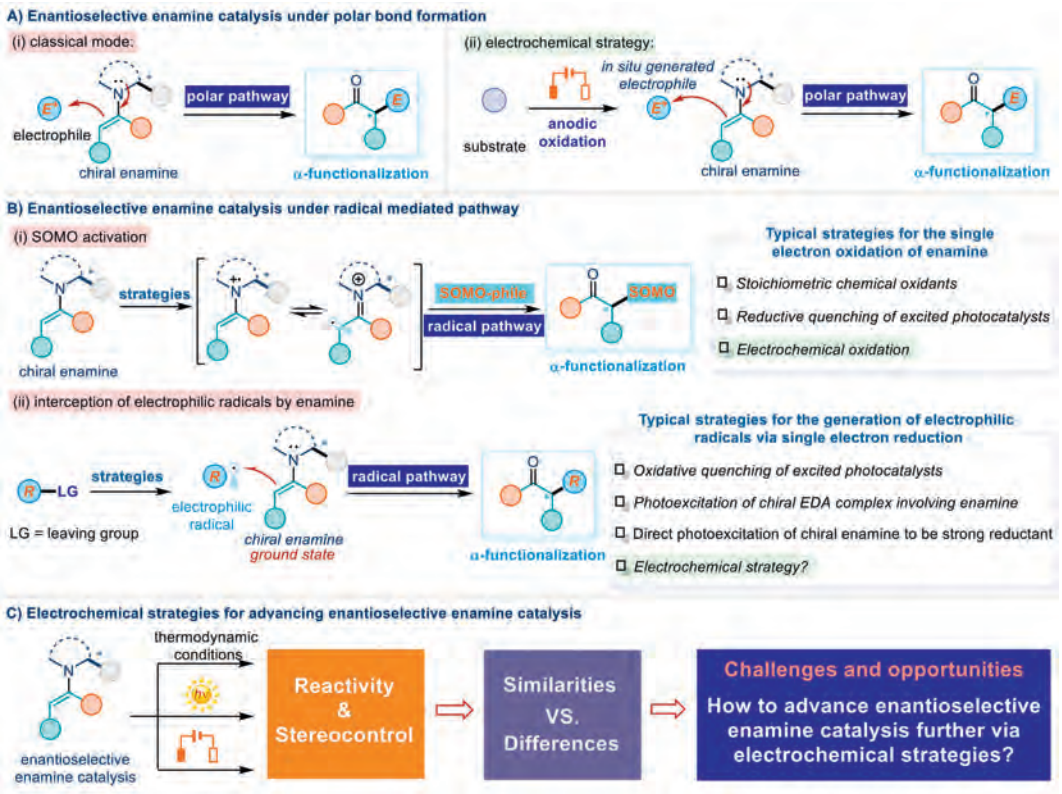


Fig. 1. Overview of enantioselective enamine catalysis.

(Fig. 1A-ii). Meanwhile, the electrochemically facilitated SOMO activation also emerged, demonstrating the capability of electrochemical methods to extend beyond conventional approaches reliant on stoichiometric chemical oxidants or photoexcited catalysts (Fig. 1B-i).

Notably, both photonic and electrical energy inputs are increasingly recognized as clean energy sources, positioned as sustainable drivers for next-generation chemical manufacturing. Significantly, the strategic integration of these energy modalities with enamine catalysis has established a continuously evolving platform for constructing chiral carbonyl compounds bearing α-stereocenters with enhanced precision and environmental compatibility. While previous reviews have systematically summarized light-mediated asymmetric enamine catalysis [19,20], electrochemical enantioselective enamine catalysis lacks integral reviews to outline its full development at this moment [45–53].

This review specifically focused on advancements in electrochemical activations concerning three principal targets (Fig. 1C): (a) Highlighting redox-stereochemical synergy within electrochemical enantioselective enamine catalysis, and pointing out crucial issues such as electrode materials, electrolyte selection, and additives in the optimization, which would be helpful for researchers to understand mechanistic paradigms and experimental challenges associated with electrochemical enantioselective enamine catalysis beyond thermodynamic and photochemical conditions; (b) Recognizing the true value of electrochemistry lies in enabling enhanced reactivities rather than mimicking traditional oxidants; (c) Inspiring potential development avenues by addressing the challenges in this area, including but not limited to the integration of electrophilic radicals with chiral enamine *via* cathodic reduction (Fig. 1B-ii).

To differentiate between electrochemical enantioselective enamine catalysis pathways, polar bond formation *versus* radical-mediated mechanisms, we provide a schematic outline prior to discussing individual reactions. The operative mechanism hinges on the oxidation state of the enamine during the key bond-forming step. When the chiral enamine has a low oxidation potential tending to be oxidized, single-electron oxidation generates a radical cation intermediate, which exists in equilibrium with the α-imino radical. Notably, the single electron oxidation occurred either at the anode or initiated by the redox mediator/shuttle homogeneously. In this scenario, the α-imino radical intermediate reacts with SOMO-philes to afford the product *via* a radical-mediated pathway. Key mechanistic identification methods include: Cyclic voltammetry (CV) revealing a low oxidation potential for the enamine, signifying its susceptibility to oxidation; Radical scavengers (*e.g.*, BHT, O_2) suppressing or halting product formation; Radical clock experiments using β-cyclopropyl-substituted carbonyls, evidenced by cyclopropane ring-opening; Exclusion studies directly reacting the enamine with potential electrophiles, and no product formation under this condition makes a polar pathway less likely (Fig. 2a).

Following a subsequent single-electron oxidation, the α-imino radical intermediate converts to an α-imino cation intermediate. This electrophilic intermediate then couples with diverse nucleophiles *via* an S_N1 pathway, representing a polar bond-formation process involving the enamine species. Key mechanistic evidence includes: Radical clock experiments using β-cyclopropyl-substituted carbonyls, where the absence of cyclopropane ring-opening would support this mechanism; Catalysts or conditions for SOMO-activation failed to afford the target products in this scenario would also provide positive mechanistic support; Mass spectrometric detection of α-imino cation intermediates or their nucleophile adducts; Kinetic studies could bring additional mechanistic insights (Fig. 2b).

When other compounds in the electrochemical cell with significantly lower oxidation potentials are present, the chiral enamine remains in its neutral form. Under these conditions, two dis-

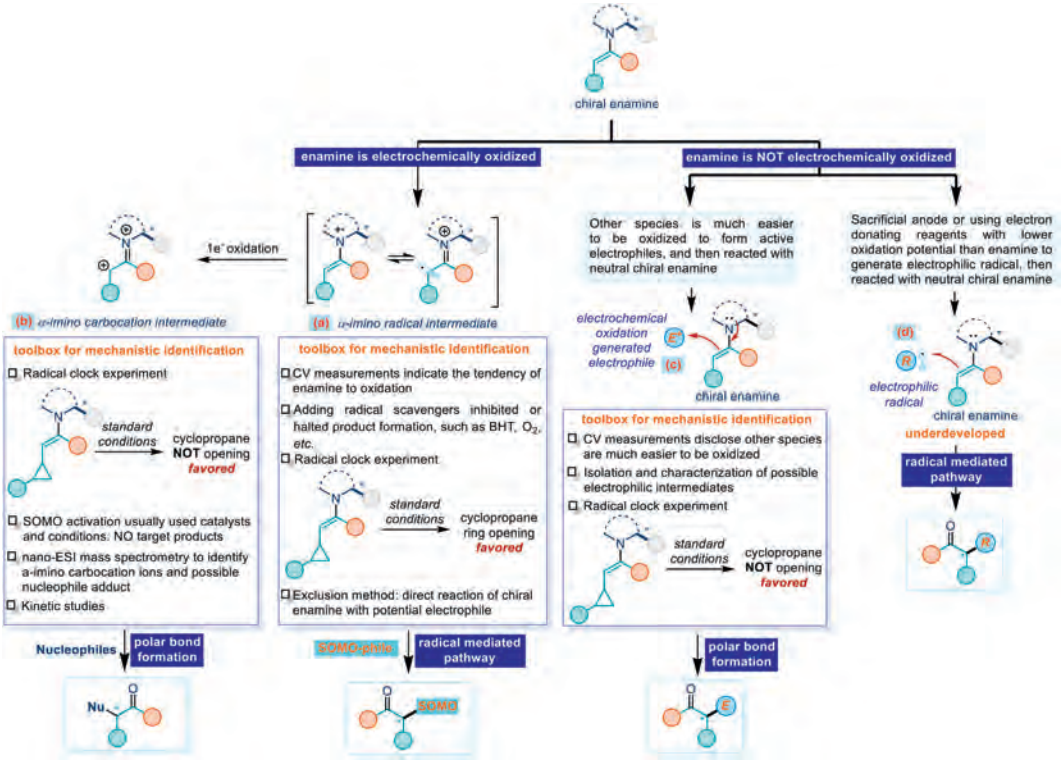


Fig. 2. Mechanistic distinctions between polar and radical-mediated pathways in electrochemical enantioselective enamine catalysis.

tinct reaction modes emerge. On one side, reagents undergo successive/multiple electron oxidation to generate active electrophilic species. These are then captured by the neutral enamine through polar bond formation, yielding the product. The aminocatalyst provides a well-defined chiral environment, ensuring highly stereoselective coupling. Within this reaction mode, several methods would be helpful for the mechanistic investigation: CV tests could recognize the species more susceptible to oxidation than enamine; Isolation and characterization of any potential electrophilic intermediates would be direct evidence; Radical clock experiments with β-cyclopropyl carbonyl compounds show absence of ring-opening, supporting non-radical mechanism (Fig. 2c).

On the other side, electrophilic radicals might be generated from corresponding precursors *via* electrochemical reduction promoted by sacrificial anode or anodic oxidation of electron donating reagents featuring lower oxidation potential than enamine. Next, this electrophilic radical could be trapped by the native enamine *via* a radical mediated pathway to yield α-functionalized products. However, this mechanistic proposal under electrochemical conditions remains underdeveloped, with stereoselectivity challenges requiring further validation (Fig. 2d). Notably, the following reactions all use undivided cells, and this will not be repeated in each reaction description.

2. Polar bond formations

In contemporary electrochemical enantioselective catalysis mediated by enamine catalysis, the predominant paradigms continue to involve coupling the native enamine species with electrogenerated electrophiles through anodic oxidation. However, this approach presents critical challenges in maintaining the oxidative stability of reaction components, particularly the aminocatalysts and chiral enamine intermediates [54,55], which requires careful evaluation during electrochemical system design. Notably, while the polar bond formation and stereocontrol mechanism have been

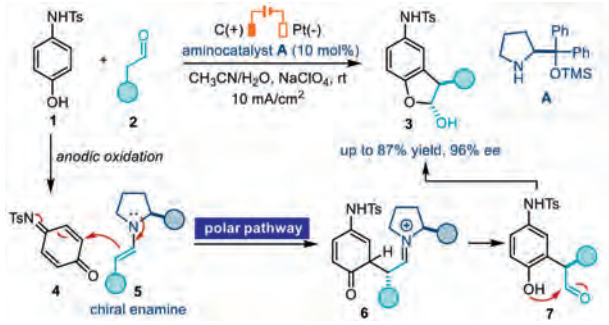
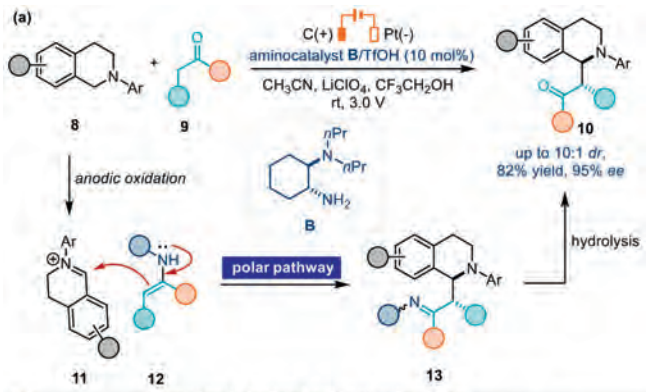


Fig. 3. Electrochemical enantioselective synthesis of *meta*-alkylated anilines *via* organocatalytic α-arylation of enamine.

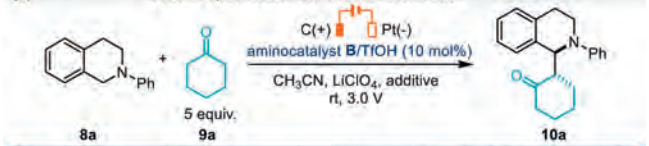
considered quite reliable in conventional thermodynamic processes, its efficacy in electro-chemical environments demands re-examination. The following successful case studies demonstrate the enduring potential of the polar pathway in modern electrochemical transformations.

In 2010, Jørgensen's group reported an electrochemical enantioselective synthesis of *meta*-alkylated anilines *via* organocatalytic α-arylation of enamine [56]. Mechanistically, it is the *N*-(4-hydroxyphenyl)-4-methylbenzenesulfonamide **1** to undergo anodic oxidation to yield electrophilic intermediate **4**, then reacted with chiral enamine **5** to afford intermediate **6**. Subsequent isomerization and hydrolysis would form **7**. Finally, hemi-acetal product **3** could be generated and isolated through intramolecular cyclization of **7**. Notably, the key bond formation step proceeds through a polar process (Fig. 3).

After that, Luo's group reported an electrochemical oxidative cross-dehydrogenative coupling reaction of tetrahydroisoquinoline **8** and simple ketone **9** to afford C1-alkylated tetrahydroisoquinoline derivatives **10** in high enantioselectivity in 2017 [57]. Cyclic



(b) Crucial optimization for this transformation



Entry	Additive	Conversion (%)	Yield (%)	*dr*	*ee* (%)
1	none	95	38	5:1	93
2	H_2O (5 equiv.)	99	65	5:1	95
3	H_2O (5 equiv.), under N_2	99	75	4:1	94
4	CF_3CH_2OH (0.02 mL), under N_2	99	75	5:1	95
5	HFIP (0.02 mL), under N_2	99	32	3:1	89

Fig. 4. Electrochemical oxidative cross-dehydrogenative coupling of tetrahydroisoquinoline and simple ketones.

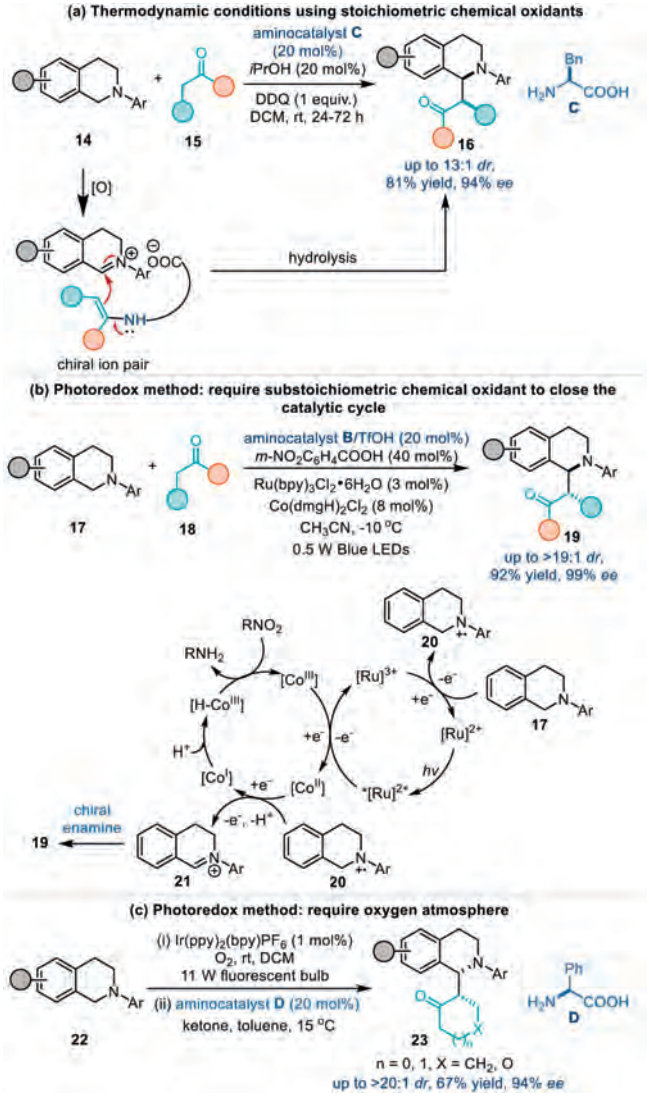


Fig. 5. Enantioselective cross-dehydrogenative coupling of tetrahydroisoquinoline and simple ketones enabled by thermodynamic and photoredox conditions.

voltammetry measurements and other control experiments indicated that tetrahydroisoquinoline **8** was transferred to active iminium ion intermediate **11** *via* anodic oxidation, ensuring a following stereoselective capture by chiral enamine **12** to give the final product **10**. In this case, the crucial bond construction step is also a polar pathway (Fig. 4a).

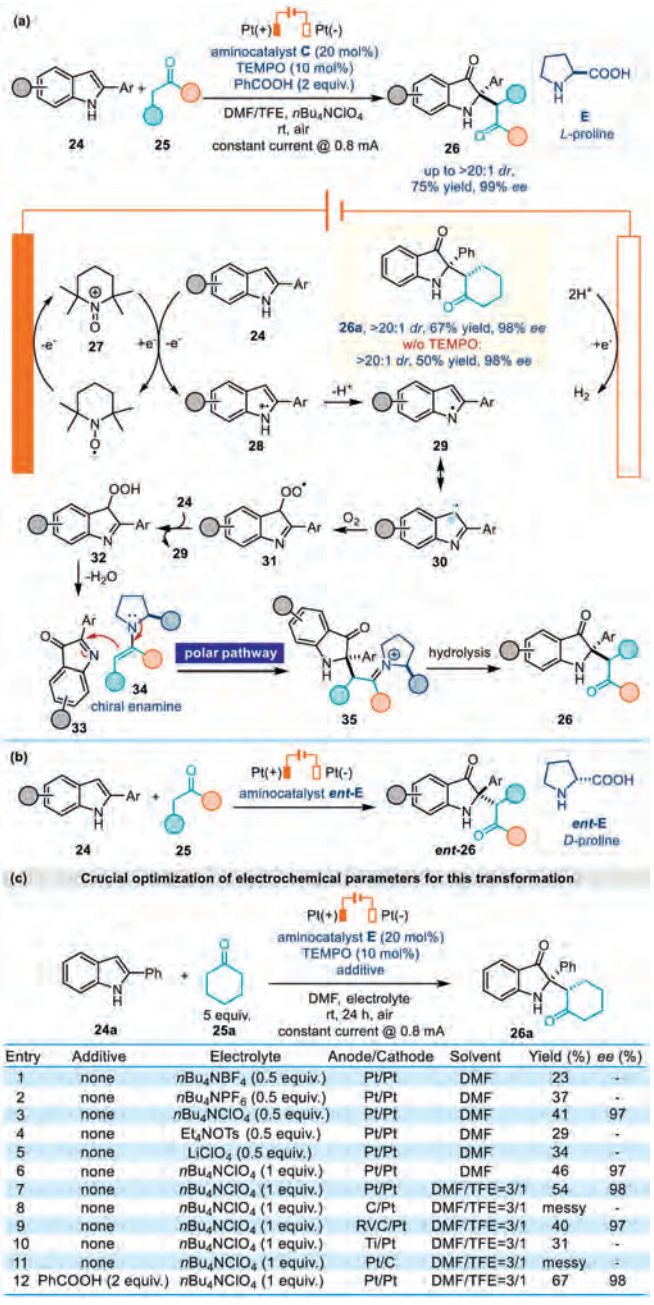
In the initial optimization, the authors observed high conversion but low yield (Fig. 4b, entry 1). Subsequently, various protonic additives were evaluated to improve efficiency. These additives potentially serve two functions: stabilizing the *in situ* generated iminium ion intermediate through hemiaminal formation [58,59], and enhancing conductivity *via* the cathodic hydrogen evolution. Upon adding 5 equiv. of water, the yield increased to 65 % (Fig. 4b, entry 2). Further optimization under a N_2 atmosphere afforded a higher yield of 75 %, albeit with slightly reduced *dr* and *ee* values (Fig. 4b, entry 3). Ultimately, CF_3CH_2OH proved most effective, while 1,1,1,3,3,3-hexafluoroisopropanol (HFIP) was less effective (Fig. 4b, entries 4 and 5).

As a comparison, this transformation was reported by Wang *et al.* using stoichiometric DDQ as the chemical oxidant in combination with chiral amino acid catalyst **C**, proposed to proceed *via* an enamine-involved chiral ion pair pathway (Fig. 5a) [60]. In 2017, Wu and Luo developed a photoredox approach employing synergistic triple catalysis (enamine/Ru/Co), where substoichiometric *m*-nitrobenzoic acid was required for cobalt cycle completion (Fig. 5b) [61]. Subsequently, Rueping *et al.* reported an alternative photoredox system using catalytic aminocatalyst **D** to deliver moderate yields with good enantioselectivity. In this reaction, an oxygen atmosphere was required (Fig. 5c) [62].

C2-fully substituted indolin-3-ones are important scaffolds in many natural products. He's group developed an electrochemical enantioselective construction of indolin-3-ones **26** bearing 2-quaternary stereocenters in high diastereoselectivity and enantioselectivity *via* organocatalytic enamine catalysis from 2-aryl indole **24** and simple ketone **25** (Fig. 6a) [63]. Mechanistic experiment revealed that 3*H*-indol-3-one **33** was a possible electrophilic intermediate to react with chiral enamine **34**, affording intermediate **35** through polar process. Final hydrolysis of **35** would provide the expected product **26**. In addition, control experiment indicated that the TEMPO additive was helpful to improve the yield of **26a** from to 50 % to 67 %. Therefore, a plausible mechanism was then proposed in combination with the cyclic voltammetry measurements. It is the TEMPO to undergo single electron oxidation at the anode to form $TEMPO^+$ **27** firstly, and then indole substrate **24** was oxidized by $TEMPO^+$ through SET (single electron transfer) to yield **28**. After losing a proton, radical intermediate **29** and its resonance **30** were generated.

Meanwhile, O_2 is proved to be quite important for this reaction since the yield of **26a** would drop significantly in argon atmosphere. The authors inferred that the oxygen of product **26a** might come from O_2 in the air atmosphere. And this hypothesis was then confirmed by $^{18}O_2$ labelling experiment. Thus, radical intermediate **30** should react with O_2 next to afford radical intermediate **31**, followed by the HAT (hydrogen atom transfer) from indole **24** to give intermediate **32**, together with the generation of intermediate **29**. Subsequent elimination of water from **32** would yield the key electrophile **33**.

Notably, catalytic employment of D-proline (*ent*–**E**) enabled stereodivergent synthesis of the enantiomers of product **26**



Entry	Additive	Electrolyte	Anode/Cathode	Solvent	Yield (%)	ee (%)
1	none	nBu_4NBF_4 (0.5 equiv.)	Pt/Pt	DMF	23	-
2	none	nBu_4NPF_6 (0.5 equiv.)	Pt/Pt	DMF	37	-
3	none	nBu_4NClO_4 (0.5 equiv.)	Pt/Pt	DMF	41	97
4	none	Et_4NOTs (0.5 equiv.)	Pt/Pt	DMF	29	-
5	none	$LiClO_4$ (0.5 equiv.)	Pt/Pt	DMF	34	-
6	none	nBu_4NClO_4 (1 equiv.)	Pt/Pt	DMF	46	97
7	none	nBu_4NClO_4 (1 equiv.)	Pt/Pt	DMF/TFE=3/1	54	98
8	none	nBu_4NClO_4 (1 equiv.)	C/Pt	DMF/TFE=3/1	messy	-
9	none	nBu_4NClO_4 (1 equiv.)	RVC/Pt	DMF/TFE=3/1	40	97
10	none	nBu_4NClO_4 (1 equiv.)	Ti/Pt	DMF/TFE=3/1	31	-
11	none	nBu_4NClO_4 (1 equiv.)	Pt/C	DMF/TFE=3/1	messy	-
12	PhCOOH (2 equiv.)	nBu_4NClO_4 (1 equiv.)	Pt/Pt	DMF/TFE=3/1	67	98

Fig. 6. Diastereo- and enantio–selective electrosynthesis of indolin-3-ones with 2-quaternary stereocenters.

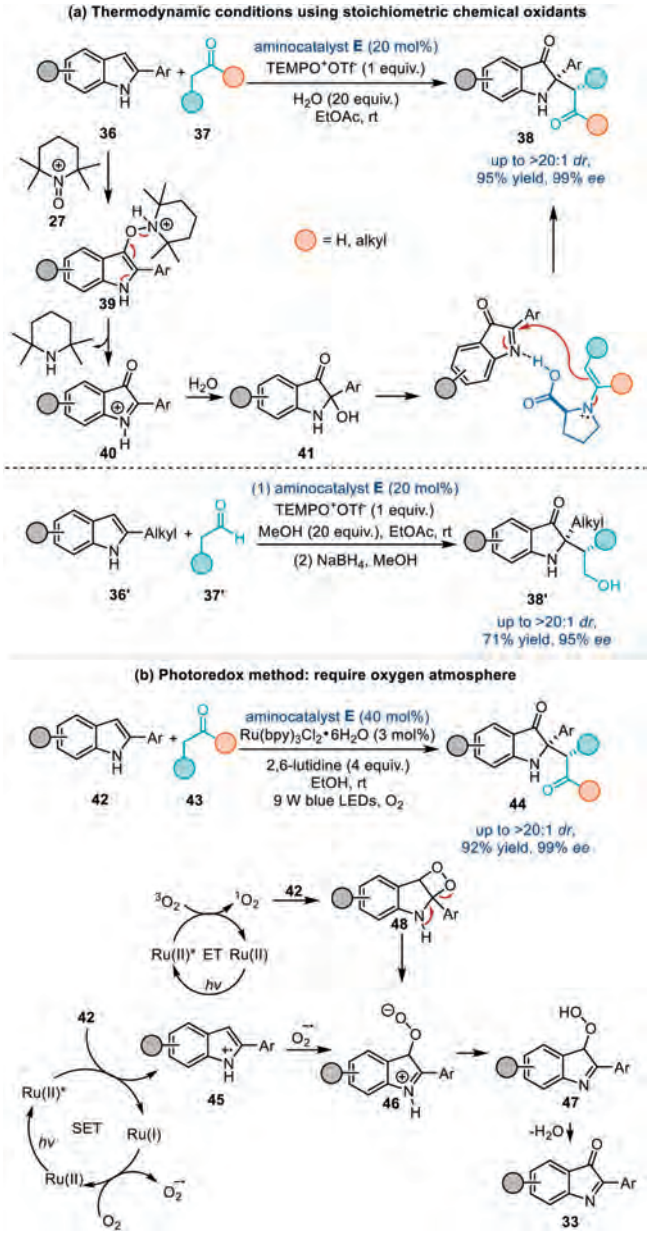


Fig. 7. Diastereo- and enantio–selective synthesis of indolin-3-ones with 2-quaternary stereocenters enabled by thermodynamic and photoredox conditions.

(Fig. 6b). This achievement not only establishes configurational diversity in C2-fully substituted indolin-3-one systems but also critically validates the robustness of the stereocontrol paradigm under electrochemical conditions.

When optimizing conditions, electrochemical parameters, specifically the electrolyte and electrodes, significantly influenced the outcome (Fig. 6c). Among those screened, nBu_4NClO_4 proved optimal as the electrolyte (Fig. 6c, entries 1–5), while Pt electrodes for both anode and cathode delivered superior results (Fig. 6c, entries 7–11). Employing a mixed DMF/TFE solvent system increased the yield (Fig. 6c, entries 6 and 7). Finally, adding PhCOOH further improved the yield to 67 % (Fig. 6c, entry 12), probably by promoting enamine formation and providing protons for hydrogen evolution at the cathode.

Prior to the development of electrochemical methods, thermodynamic methods and photoredox catalysis have demonstrated their ability to promote this type of transformation. Notably, stoichiometric $TEMPO^+OTf^-$ was employed to form the crucial intermediate **40** [64], which could also generate the hemiaminal intermediate **41** in the presence of water (Fig. 7a). The photochemical reaction, meanwhile, was conducted under an oxygen atmosphere with an elevated loading of aminocatalyst **E** [65]. The same electrophilic species **33** was formed either by single-electron reduction of oxygen gas to superoxide anion or *via* energy transfer (ET)-enabled [2 + 2] cycloaddition of singlet oxygen with indole reactants (Fig. 7b).

In 2020, Luo and colleagues reported a groundbreaking electrochemical strategy for the asymmetric α-arylation of cyclic β-ketocarbonyls using enamine catalysis (Fig. 8a) [66]. Central to this methodology was the *in situ* electrochemical generation of reactive benzyne **52**, which proved critical for achiev-

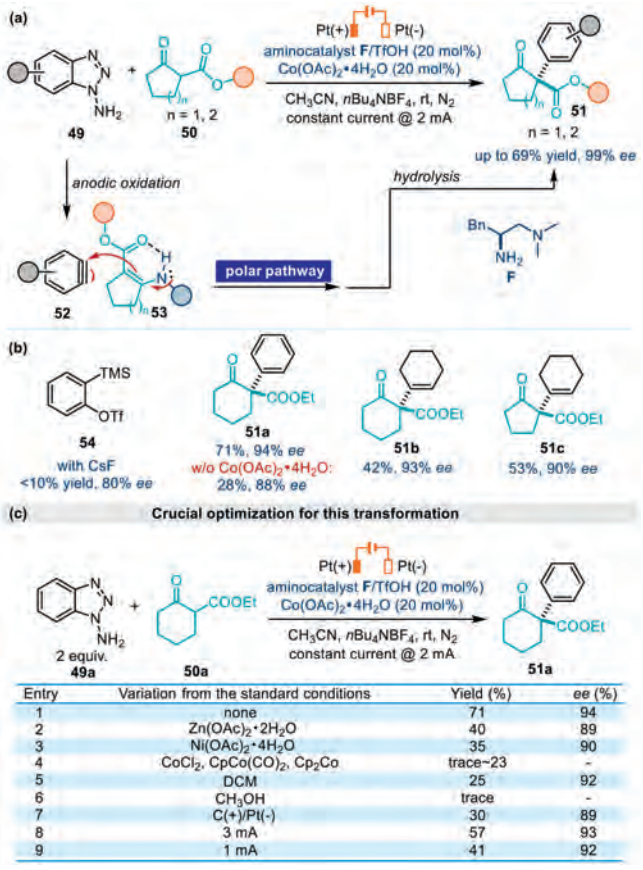


Fig. 8. Electrochemically enabled asymmetric α-arylation of cyclic β-ketocarbonyl compounds *via* enamine catalysis.

ing high reaction efficiency. Conventional approaches employing 2-(trimethylsilyl)phenyl triflate **54** as a benzyne precursor under thermodynamic conditions could only yield <10% product, underscoring the superiority of the electrochemical protocol. Mechanistically, anodic oxidation of 1-aminobenzotriazole **49** generated benzyne **52**, which underwent stereoselective polar C–C bond formation with chiral enamine intermediate **53** to deliver product **51** with excellent enantioselectivity.

Cyclic voltammetry analysis rationalized the chemo-selectivity: 1-aminobenzotriazole **49a** ($E_{ox} = 0.84$ V) exhibited significantly lower oxidation potential compared to both the aminocatalyst ($E_{ox} = 1.54$ V) and enamine intermediate ($E_{ox} = 1.15$ V), ensuring preferential benzyne generation. The catalytic system further required $Co(OAc)_2 \cdot 4H_2O$ as a crucial additive, with control experiments demonstrating a dramatic decline in yield (28% *vs.* 71%) and slightly lower enantioselectivity (88% *ee vs.* 94% *ee*) in its absence (Fig. 8b). Benzyne quenching studies and DFT calculation suggested cobalt's role in stabilizing the transient aryne intermediate through triple-bond coordination.

Notably, apart from the capture of benzyne intermediate, α-vinylated products **51b** and **51c** could also be afforded starting from corresponding cyclic alkyne precursors in moderated yields and excellent *ee* values (Fig. 8b). This work establishes electrochemistry as a powerful tool for manipulating reactive intermediates in asymmetric catalysis.

Concerning the acquisition of the best conditions, metal additives (Fig. 8c, entries 2–4) and solvents (Fig. 8c, entries 5 and 6) both had an important effect. In addition, changing the anode material to graphite (Fig. 8c, entry 7), and varying currents (Fig. 8c, entries 8 and 9) all result in obviously diminished yields.

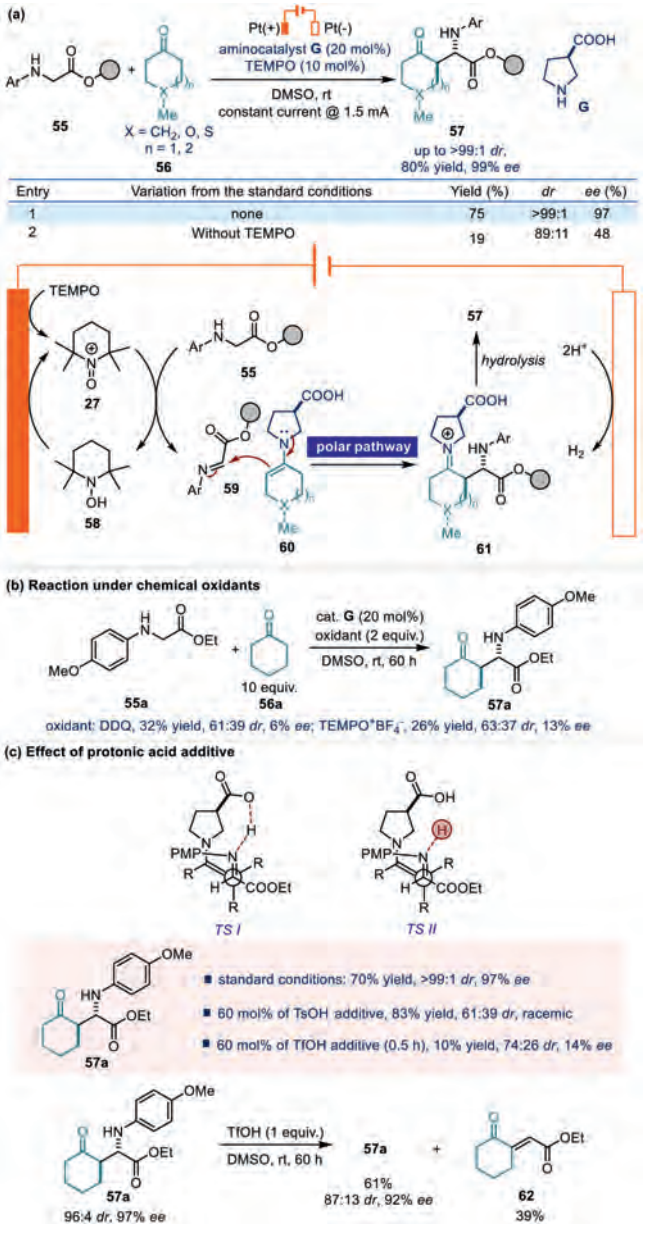


Fig. 9. TEMPO mediated electrochemical stereoselective Shono-type cross dehydrogenative coupling of acyclic amines and cyclic ketones.

In 2021, Mei's team successfully realized the stereoselective Shono-type cross dehydrogenative coupling of acyclic amines and cyclic ketones by employing TEMPO as a redox mediator (Fig. 9) [54]. Notably, a suitable redox mediator was proved to be able to accelerate the electron transfer on the electrode surface, thus enables the electrochemical transformation at a lower oxidative potential, enhancing the overall efficiency and feasibility of the reaction process [39,67–69].

The crucial role of TEMPO in this reaction could be verified by the control experiment in the absence of it, which resulted in a significantly lower yield, as well as diastereo- and enantioselectivity (Fig. 9a). Meanwhile, cyclic voltammetry experiments also elucidated the mediator role of TEMPO. Based on these experimental findings, a plausible reaction mechanism was proposed. Initially, TEMPO undergoes single-electron oxidation at the anode to form the intermediate **27**. Subsequently, **27** oxidizes glycine ester **55**, yielding the electron-neutral imine intermediate **59**. Following this, the nucleophilic addition of a chiral enamine to intermediate **59**

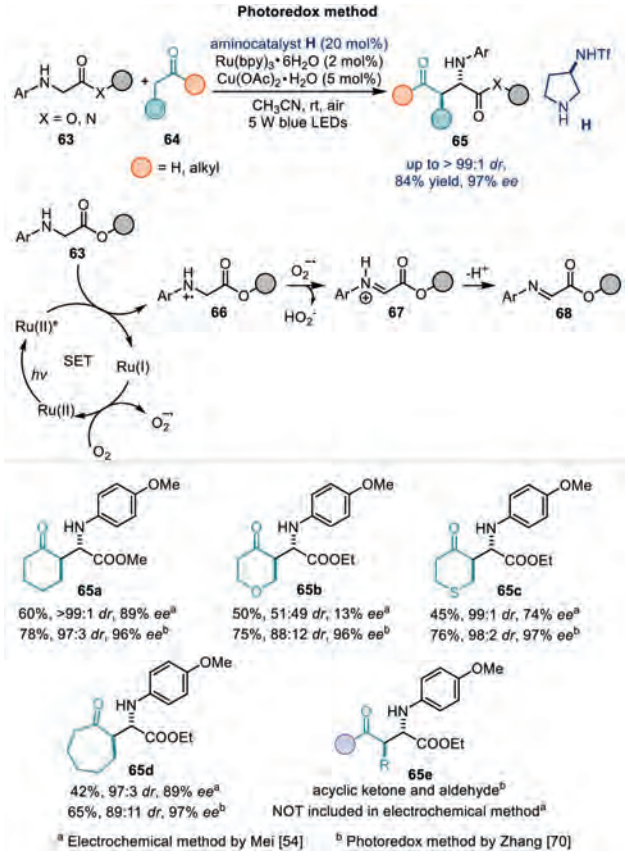


Fig. 10. Photoredox cross-dehydrogenative coupling of glycine derivatives with ketones and aldehydes.

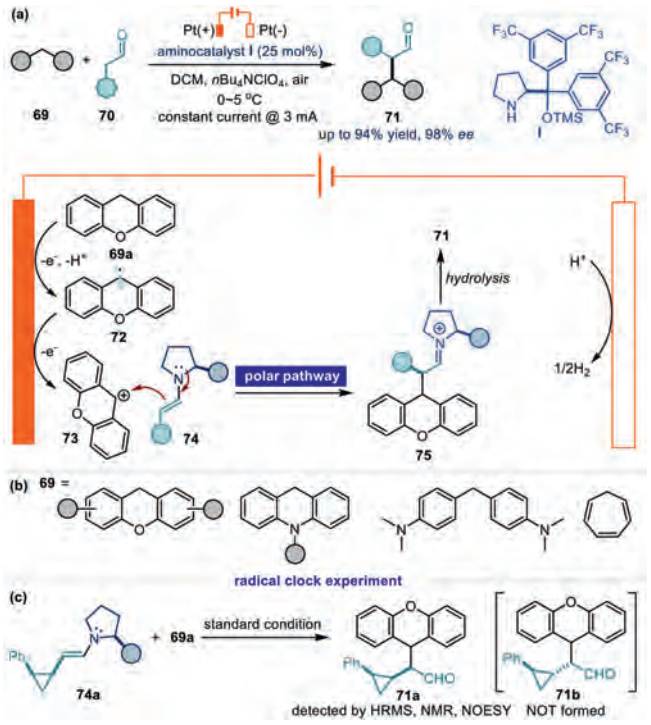


Fig. 11. Enantioselective electrochemical cross-dehydrogenative coupling of aldehydes and benzylic C(sp^3)-H bonds.

generates intermediate **61.** Ultimately, the hydrolysis step affords the target product **57** with high diastereo- and enantioselectivity. Moreover, it is noteworthy that the key C–C bond connection step in this transformation follows a polar pathway.

The significant advantages of the electrochemical strategy in this transformation are further highlighted by comparative studies. When chemical oxidants such as DDQ or $TEMPO^+BF_4^-$ were used instead of the electrochemical approach, the resulting products exhibited considerably lower diastereo- and enantioselectivity (Fig. 9b). Furthermore, the authors propose that a hydrogen bonding interaction between the acidic proton of chiral aminocatalyst **G** and the imine is crucial for achieving high enantioselectivity (*TS-I*, Fig. 9c). In contrast, alternative proton sources, such as protons generated from glycine ester **55** oxidation under thermodynamic conditions using chemical oxidants, could induce racemization due to competing interactions (*TS-II*, Fig. 9c). Further mechanistic investigations, including studies on the effects of proton additives and the stability of the products under acidic conditions, supported the above proposal and revealed that the key to the success of this protocol lies in the hydrogen evolution occurring at the cathode to efficiently decline the effect of proton on the stereoselective outcomes (Fig. 9c).

This transformation was also achieved *via* photoredox catalysis using molecular oxygen, facilitating the formation of the electrophilic imine intermediate **68** [70]. For comparison, representative examples were selected to illustrate the differences between the two approaches (Fig. 10). In some cases, the electrochemical method afforded superior diastereoselectivity, while the photochemical method provided higher yield and enantioselectivity. Furthermore, acyclic ketones and aldehydes proved suitable under photoredox conditions, which were not reported by Mei *et al.* [54]. Therefore, not all electrochemical transformations surpass existing methods at this stage, thus there remains significant spaces for improvement in electrochemical enantioselective enamine catalysis.

Pan's group has reported an innovative enantioselective electrochemical cross-dehydrogenative coupling reaction involving active benzylic C(sp^3)-H bonds with aldehydes in 2024 (Fig. 11a) [71]. This reaction proceeds *via* the stereoselective capture of carbocation species generated by anodic oxidation, using enamines as nucleophiles in a polar manner. The versatility of this method is further demonstrated by the successful use of alternative coupling partners, including xanthene, methylacridine, diarylmethane, and cycloheptatriene (Fig. 11b).

The electrochemical conditions employed in this study have been well optimized to ensure superior enantioselectivity control compared to previous reports [72]. Mechanistically, taking xanthene as an example, the compound **69a** exhibits a lower oxidation potential (1.15 V *vs.* Ag/AgCl) than both the aldehyde and the corresponding enamine intermediate, as evidenced by cyclic voltammetry studies. Moreover, a radical clock reaction using **74a**, derived from a *cis*-cyclopropyl-substituted aldehyde exclusively yielded product **71a** with a *cis*-substituted cyclopropane under the electrochemical conditions (Fig. 11c). This outcome further supports the proposed mechanism involving the selective oxidation of **69a** to **73** *via* twice single electron oxidation and subsequent capture by the enamine *via* polar bond formation mechanism. This detailed mechanistic understanding not only validates the proposed reaction pathway but also underscores the robustness and precision of the electrochemical approach in achieving high enantioselectivity.

In a 2024 report, Xu and coworkers also brought an electrochemical cross-dehydrogenative coupling strategy for the α-alkylation of aldehydes using 9,10-dihydroacridines [73]. Distinct from Pan's work, this system employed catalytic TEMPO as a redox mediator to facilitate single-electron oxidation of dihydroacridine **76**, generating radical cation intermediate **79**. Subsequent reaction with O_2 produced iminium ion intermediate **80**, which served as

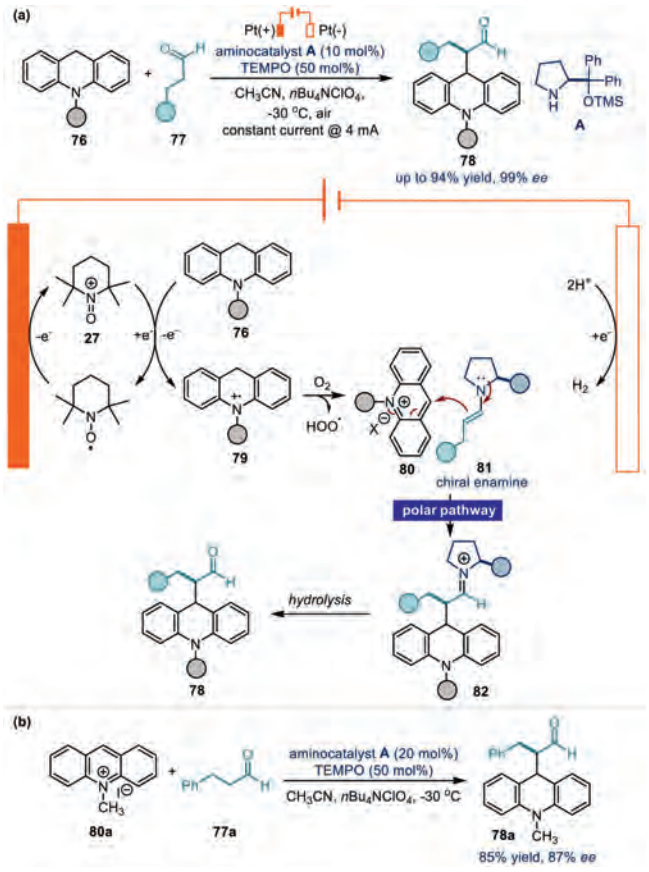


Fig. 12. Enantioselective electrochemical α-alkylation of aldehydes using 9,10-dihydroacridines.

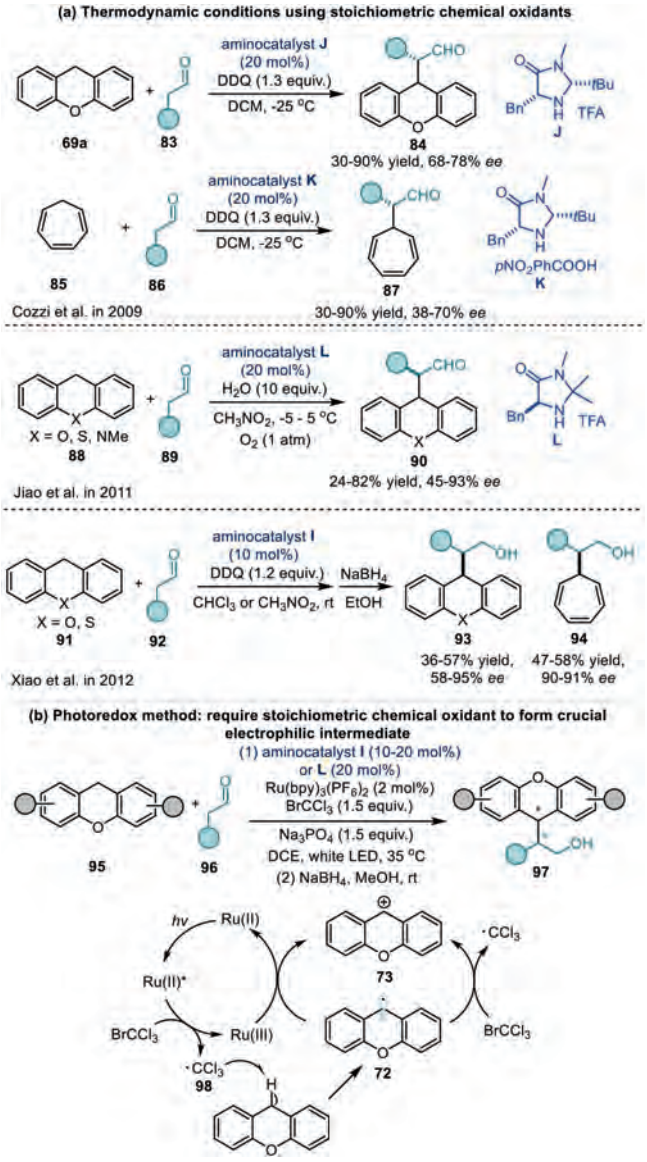


Fig. 13. Enantioselective dehydrogenative α-alkylation of aldehydes enabled by thermodynamic and photoredox conditions.

the critical electrophile for stereoselective trapping by chiral enamine **81** (Fig. 12a). Mechanistic validation included control experiments with pre-synthesized **80a**, confirming the intermediacy of the iminium species (Fig. 12b). Notably, the crucial C–C bond formation step was identified as a polar process.

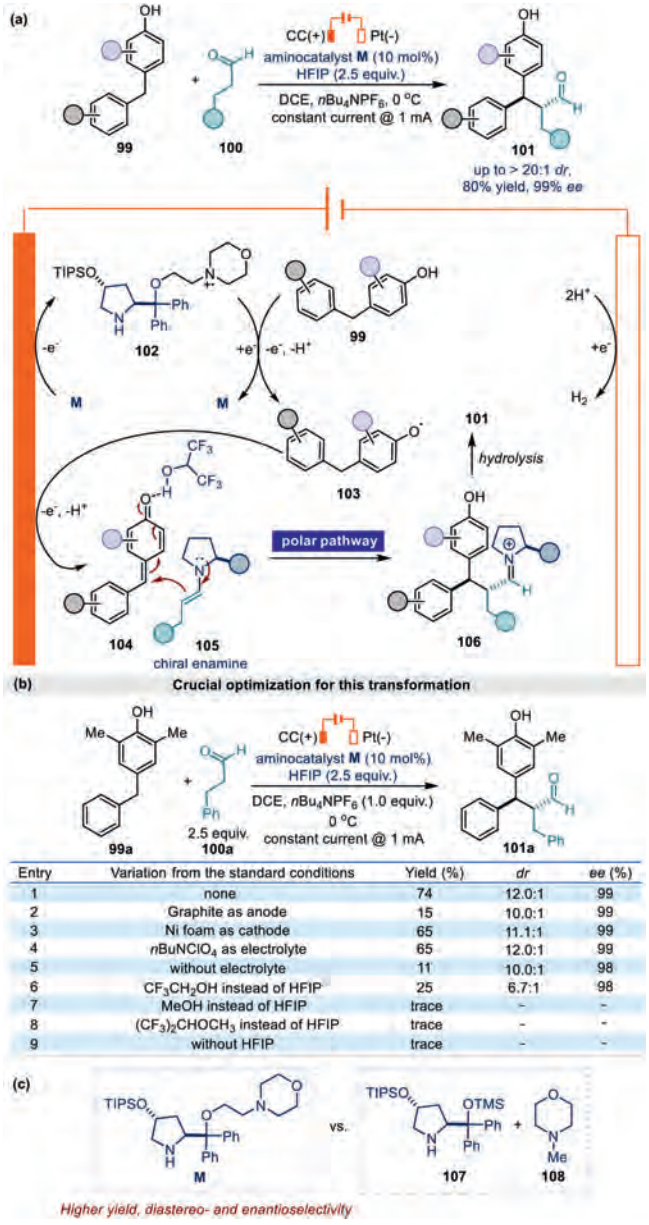
Correspondingly, chemical oxidants, such as DDQ and molecular oxygen were also compatible for this reaction as reported by Cozzi [74], Jiao [75] and Xiao (Fig. 13a) [76]. Within the photochemical transformation developed by Pericàs [77], a stoichiometric oxidant $BrCCl_3$ was still required to generate the crucial carbocation intermediate **73** (Fig. 13b).

Meanwhile, Xu and coworkers reported an electrochemical enantioselective α-alkylation of aldehydes utilizing a newly designed bifunctional chiral aminocatalyst (Fig. 14a) [78]. The key innovation lies in the integration of a tertiary amine redox mediator moiety into a pyrrolidine-based chiral catalyst framework. This dual-functional design synergistically combines efficient electron transfer mediation with stereochemical control, providing a paradigm for achieving both high efficiency and enantioselectivity in electrochemical asymmetric catalysis.

After systematic optimization, catalyst **M** was proven to be the optimal from two aspects: (i) Acting as a redox mediator for the efficient oxidation of phenol **99** to radical intermediate **103** as confirmed by CV measurements. Then **103** was oxidized further at the anode to yield electrophilic *para*-quinone methide intermediate **104**. (ii) The *in situ* generated chiral enamine **105** from catalyst **M** underwent nucleophilic addition to **104**, affording intermediate **106**, which finally led to product **101** through hydrolysis.

Detailed reaction optimization established the optimal conditions: carbon cloth anode, platinum cathode, nBu_4NPF_6 electrolyte, HFIP additive in DCE at 0 °C under constant current (1 mA). Substituting the anode with graphite or the cathode with Ni foam afforded inferior results (Fig. 14b, entries 2 and 3). Similarly, using nBu_4NClO_4 as electrolyte yielded only 65 % product (Fig. 14b, entry 4). The electrolyte proved essential, as its absence reduced the yield to 11 % (Fig. 14b, entry 5). Importantly, HFIP was critical for high efficiency, substitutes such as CF_3CH_2OH, MeOH, or $(CF_3)_2CHOCH_3$ significantly diminished reactivity (Fig. 14b, entries 6–8), while omission of HFIP almost suppressed product formation entirely (Fig. 14b, entry 9).

Mechanistic studies revealed that HFIP could activate the *para*-quinone methide *via* hydrogen bonding and help to improve the diastereocontrol to some extent owing to the steric hindrance. What's more, comparative studies highlighted the superiority of catalyst **M** over conventional systems employing separate aminocatalyst **107** and *N*-methylpiperidine **108**, with **M** consistently delivering superior yields and stereoselectivity across selected substrates (Fig. 14c). This work establishes a new thinking for merging electrochemical activation with asymmetric enamine organocatalysis through bifunctional catalyst design.

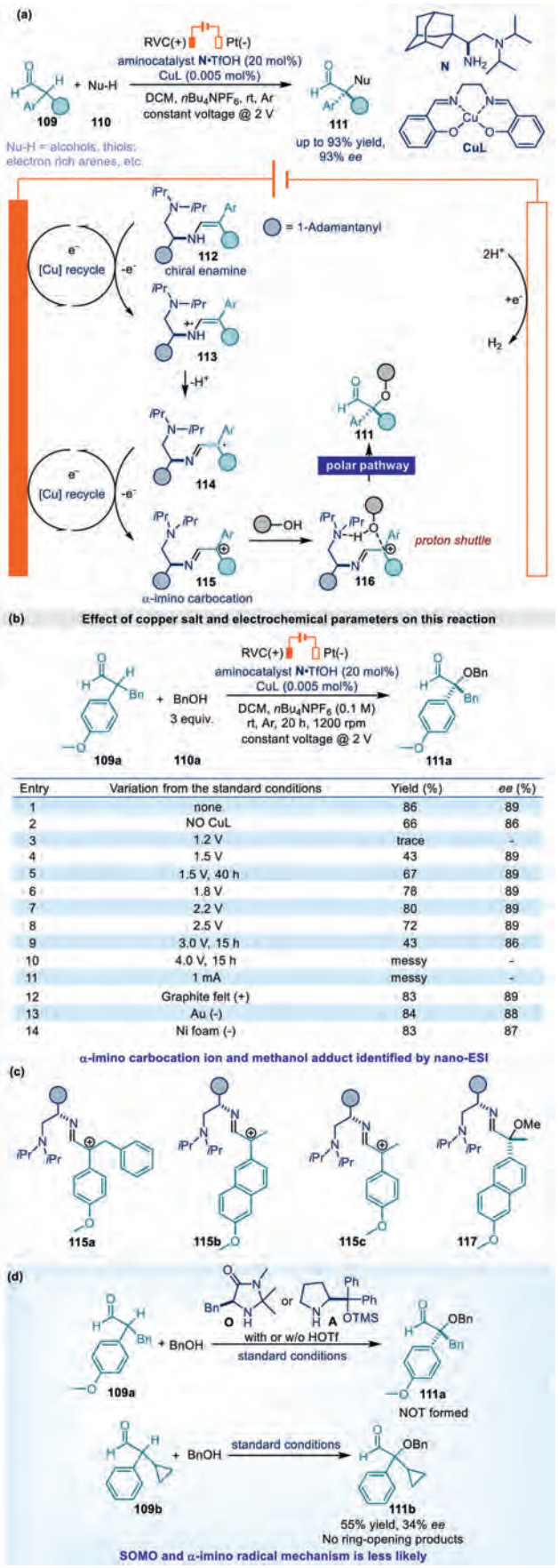


Entry	Variation from the standard conditions	Yield (%)	*dr*	*ee* (%)
1	none	74	12.0:1	99
2	Graphite as anode	15	10.0:1	99
3	Ni foam as cathode	65	11.1:1	99
4	nBuNClO$_4$ as electrolyte	65	12.0:1	99
5	without electrolyte	11	10.0:1	98
6	CF_3CH_2OH instead of HFIP	25	6.7:1	98
7	MeOH instead of HFIP	trace	-	-
8	$(CF_3)_2CHOCH_3$ instead of HFIP	trace	-	-
9	without HFIP	trace	-	-

Fig. 14. Electrochemical enantioselective α-alkylation of aldehydes using bifunctional chiral aminocatalyst.

Apart from above achievements utilizing classical enamine catalysis to catch electrochemical oxidation generated electrophiles, a novel S_N1 type α-functionalization of aldehyde was reported by Luo's group in 2024 *via* α-imino carbocation intermediate (Fig. 15a) [79]. First of all, a minuscule amount of copper additive CuL was proven effective for improving the reaction rate and final yield by control experiment (Fig. 15b, entries 1 and 2). Further mechanistic studies revealed that the most probable role of copper was acting as a redox mediator for the electrochemical oxidative generation of α-imino carbocation intermediate **115**.

Constant voltage electrolysis proved essential for this reaction. After optimization, 2.0 V afforded optimal results (Fig. 15b, entry 1). Reactions at 1.2 V failed to generate product (Fig. 15b, entry 3), while 4.0 V produced complex mixtures with unidentified side products (Fig. 15b, entry 10). Voltages between 1.5–1.8 V and 2.2–3.0 V yielded lower efficiency (Fig. 15b, entries 4–9). Similarly, constant current electrolysis at 1 mA generated messy mixtures with unknown side products (Fig. 15b, entry 11). Attempts using



Entry	Variation from the standard conditions	Yield (%)	*ee* (%)
1	none	86	89
2	NO CuL	66	86
3	1.2 V	trace	-
4	1.5 V	43	89
5	1.5 V, 40 h	67	89
6	1.8 V	78	89
7	2.2 V	80	89
8	2.5 V	72	89
9	3.0 V, 15 h	43	86
10	4.0 V, 15 h	messy	-
11	1 mA	messy	-
12	Graphite felt (+)	83	89
13	Au (-)	84	88
14	Ni foam (-)	83	87

Fig. 15. Electrochemical enantioselective α-functionalization of aldehydes *via* α-imino carbocation intermediate.

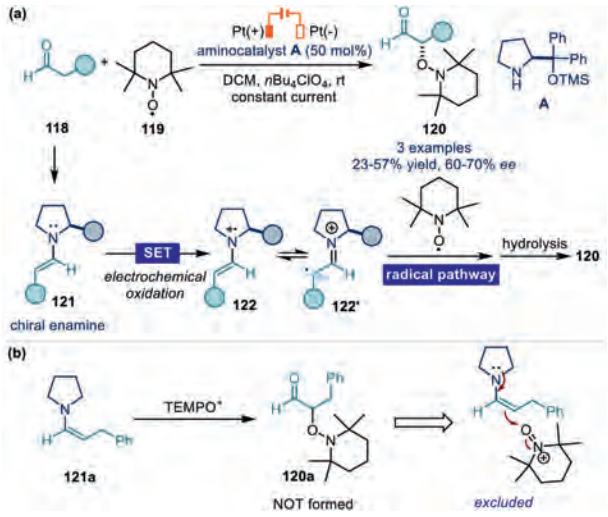


Fig. 16. Electrochemical α-oxyamination of aldehydes *via* enamine catalysis and preliminary enantioselective results.

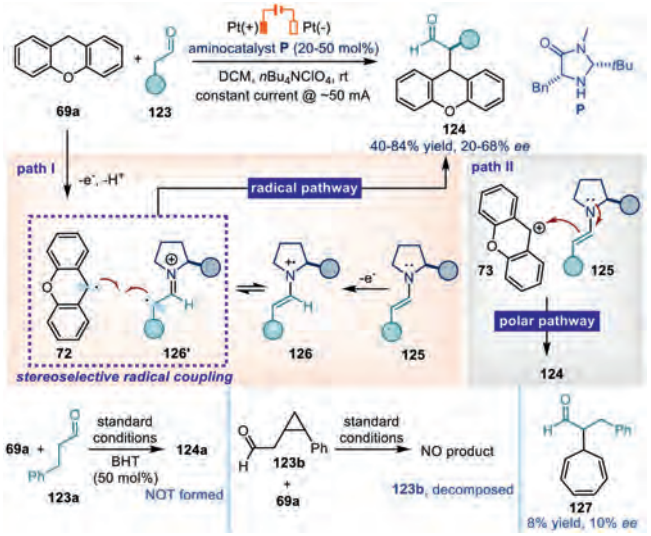


Fig. 17. Electrochemically driven enantioselective α-alkylation of simple aldehydes with xanthene.

graphite anodes or gold/nickel foam cathodes all afforded slightly reduced yields (Fig. 15b, entries 12–14).

Impressively, detailed mechanistic studies, including control experiments and kinetic investigations provide sufficient evidence for the formation of α-imino carbocation intermediate in the electrochemical system. For instance, α-imino carbocation intermediates **115a-115c** and the methanol adduct **117** could be identified by nano-ESI, demonstrating the feasibility of proposed reaction pathway (Fig. 15c). In addition, the absence of product **111a** in the reactions employing secondary chiral aminocatalysts (imidazolidinone **O** and prolinol **A**), coupled with radical clock experiments using aldehyde **109b**, helpfully excluded competing SOMO and α-imino radical mechanisms (Fig. 15d).

Besides, DFT calculations provided critical insight into stereochemical control, demonstrating that the tertiary amine moiety in catalyst **N** orchestrates hydrogen transfer in intermediate **116** as well as the hydrogen-bonding interactions. In this scenario, the key C–C and C-X bonds formation step is also a polar process. A series of alcohols, thiols, and electron rich arenes could take part in the reaction with moderate to good yield and good enantioselectivity, while trials using *N*-based nucleophiles didn't work as well as others to result in 22%–24% yield and worse enantioselectivity (33%–78% *ee*), leaving spaces for further improvement.

3. Radical mediated pathways

Comparing to above summarized asymmetric transformations enabled by electrochemical enamine catalysis with polar chemical bond building paradigm, the radical mediated examples from radical cation or α-imino radical were still less explored.

In 2009, a pioneering reaction of α-oxyamination of aldehydes enabled by electrochemical enamine catalysis came from Jang's group (Fig. 16a) [80]. Cyclic voltammetry and control experiments indicated that electrochemical oxidation generated radical cation **122** from enamine **121** was an essential active species to react with TEMPO, yielding α-oxyaminated product **120** finally. While the C–O bond formation under the classically polar mode of enamine to undergo nucleophilic addition to $TEMPO^+$ could be ruled out based on the outcomes that product **120a** could not be formed from the reaction of enamine with commercially available $TEMPO^+$ (Fig. 16b).

Further exploration of enantioselective variants demonstrated that 50 mol% of chiral aminocatalyst **A** could deliver the desired product with moderate enantioselectivity and yield. Although these stereochemical results were suboptimal, this work represented a paradigm shift by establishing the feasibility of stereoselective radical coupling with chiral enamine intermediates under electrochemical circumstance.

One year later, Jang's group reported their finding in the electrochemically driven enantioselective α-alkylation of simple aldehydes with xanthene (Fig. 17) [72]. Two mechanisms are proposed: (i) Stereoselective coupling of carbon radical **72** and α-imino radical **126′** from single electrochemical oxidation of xanthene **69a** and enamine **125**, respectively. In this hypothesis, the key C–C bond formation step is a radical pathway (Fig. 17, path I). (ii) Polar mode nucleophilic addition of enamine to carbocation intermediate **73** coming from anodic oxidation of **69a** (Fig. 17, path II). Mechanistic studies including CV test, adding radical trapping reagent BHT, as well as radical clock trial supported the radical coupling procedure. Finally, product **127** was formed in quite low yield and *ee* starting from cycloheptatriene.

Even though the enantioselectivities were not so good (20%–68% *ee*) (Fig. 17), and some of which even require substoichiometric amount of chiral catalyst (50 mol%), this preliminary result further demonstrated the stereoselectivity controllability under electrochemical conditions, which could work much better through continuously optimized conditions yet with different mechanism (Fig. 11) [71].

A highly enantioselective α-alkylation and allylation of aldehydes was accomplished by Dell'Amico *et al.* in 2024 *via* the electrochemical SOMO activation (Fig. 18a) [55]. Both the biphenyl additive **133** and water were quite essential for the expected high reactivity as the yield would drop significantly without their participations (Fig. 18b, entries 1–3). Furthermore, replacing the electrolyte to $n\text{Bu}_4\text{NBF}_4$ or $n\text{Bu}_4\text{NPF}_6$ gave 34%–61% yield compared to 70% with $n\text{Bu}_4\text{NClO}_4$ (Fig. 18b, entry 4). Meanwhile, using graphite as anode was less effective compared to reticulated vitreous carbon (RVC) (Fig. 18b, entry 5).

Control experiment, CV measurements, UV–vis absorption spectroscopy studies, cell potential monitoring, as well as the time-dependent density functional theory (TD-DFT) calculations indicated that a biphenyl additive **133** acted as a redox shuttle to inhibit the decomposition of chiral aminocatalyst, and to facilitate the single electron oxidation of enamine **134** to generate α-imino radical **135′** for an improved efficiency. Next, polarity match triggered reaction of **135′** with electron rich olefins, such as the

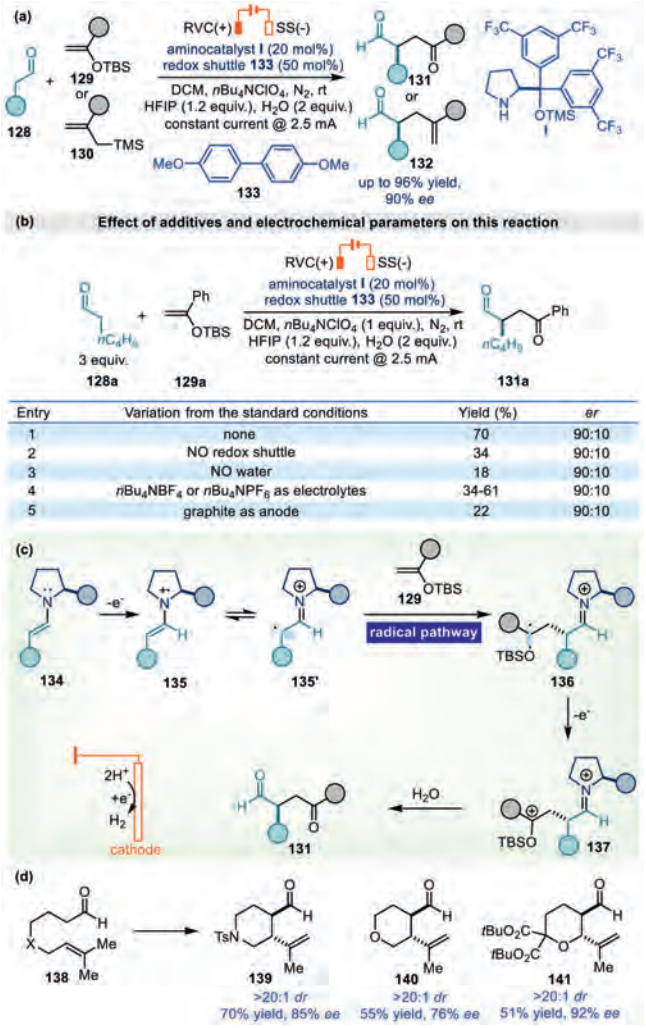


Fig. 18. Radical based electrochemical enantioselective α-alkylation and allylation of aldehydes.

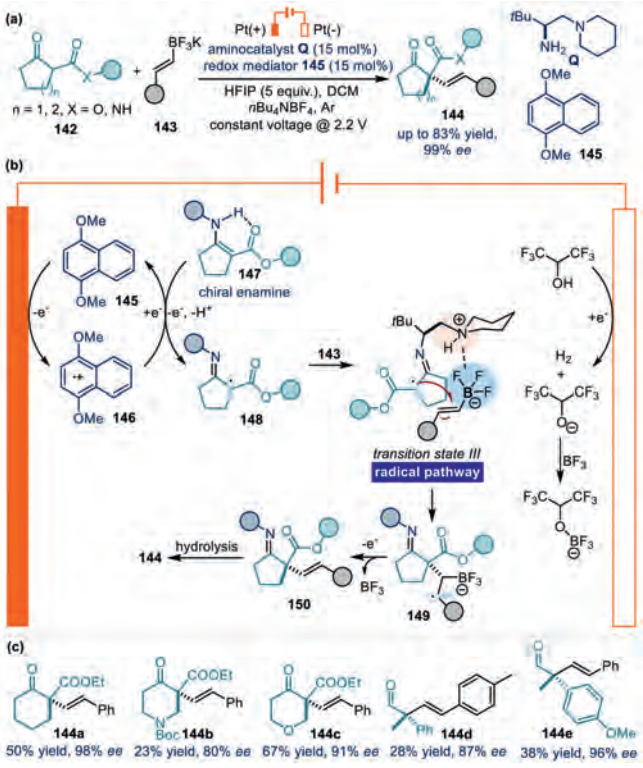


Fig. 19. Organo-mediated electrochemical enantioselective α-alkenylation of ketones *via* SOMO catalysis.

silyl enol ethers, would generate intermediate **136** following a radical mediated pathway. Subsequent oxidation and hydrolysis afforded the target chiral product (Fig. 18c). Notably, intramolecular α-allylations were also accessible to afford cycloalkanes with adjacent stereocenters in high diastereoselectivity (Fig. 18d). The success of this protocol verified that an improved stereocontrol could indeed be realized by the radical mechanism under electrochemical enamine catalysis.

Recently, Luo's team successfully move the electrochemical asymmetric SOMO activation forward to develop an α-alkenylation of ketones in high enantioselectivity *via* synergistic enamine catalysis and electrochemistry using an organic naphthalene mediator (Fig. 19a) [81]. Based on the radical trapping results and CV measurement studies, naphthalene **145** was proven to act as an efficient mediator for the smooth oxidization of chiral enamine intermediate **147** to α-imino radical intermediate **148**, ensuring an improvement of the total productivity. After that, a stereoselective C–C bond formation *via* radical process occurred through transition state *TS III*, whereas the ion-pair interaction between the protonated tertiary amine in the aminocatalyst and the anion region in the styryl trifluoroborate was identified quite important for the observed high stereoselectivity.

This scenario was also supported by the outcomes from stoichiometric reaction utilizing preprepared enamine with water additive, effect of boron groups, solvents, and tertiary amine structures within the aminocatalyst, as well as the DFT calculation analysis. Once formed, radical intermediate **149** would undergo a following single electron oxidation to give the expected product (Fig. 19b). Notably, except the five-membered cyclic β-ketoesters, six-membered cyclic β-ketoesters, and the ones with nitrogen and oxygen atoms, as well as acyclic aldehydes could all take part in the reaction to yield the target products in 23 %–67 % yields and 80 %–98 % *ee* (Fig. 19c).

4. Conclusion and outlook

In conclusion, electrochemical methodologies have emerged as a transformative platform for advancing enantioselective enamine catalysis, demonstrating dual advantages in sustainable synthesis and novel reactivity exploration. Current achievements validate their capacity to replace conventional chemical oxidants while introducing unique mechanistic dimensions, as evidenced by electricity-dependent stereochemical outcomes above. The established paradigm predominantly utilizes polar chemical bond formation through chiral enamine-mediated nucleophilic addition to electrochemically generated electrophiles. However, this technological superiority should not be misinterpreted as mere oxidant substitution, and the applied potential itself serves as an essential mechanistic variable enabling unprecedented reaction pathways.

Three critical challenges demand focused attention: (i) Oxidation sensitivity management across different components (aminocatalyst, enamine intermediate, substrates, and products), which fundamentally dictates both reaction efficiency and mechanistic feasibility; (ii) Improving compatibility of classical stereocontrol strategies with complex electrochemical environments. Encouragingly, these achievements have preliminarily established reliable frameworks for asymmetric control *via* both polar processes (transient electrophiles) and radical mechanisms (radical species).

Future development could prioritize: (i) Expansion beyond current electro-oxidative dominance to encompass reductive radical pathways, such as the α-functionalization *via* electroreductively generated electrophilic radicals, as exemplified in Fig. 1B-ii through photocatalytic prototypes. (ii) *De novo* design of stereocontrol strategies leveraging electrochemical resolution. (iii) Integration of advanced characterization techniques for real-time mechanistic elucidation.

The demonstrated successes, while significant, merely outline the preliminary chapter in what promises to be a transformative approach to asymmetric synthesis. We anticipate that the synergistic integration of electrochemical evolution with enamine catalysis will drive the emergence of innovative catalytic paradigms, potentially revolutionizing modern synthetic methodologies through unprecedented reaction pathways and selectivity control.

Declaration of competing interest

The authors declare that they have no known competing financial interests or personal relationships that could have appeared to influence the work reported in this paper.

CRediT authorship contribution statement

Dengke Ma: Writing – review & editing, Writing – original draft, Visualization, Validation, Funding acquisition, Conceptualization. **Youai Qiu:** Writing – review & editing, Validation, Conceptualization.

Acknowledgments

Financial support from National Natural Science Foundation of China (No. 22201187), and the starting grant from Capital Medical University (No. 3100–12500121) are gratefully acknowledged.

References

[1] C.C.C. Johansson, T.J. Colacot, Angew. Chem. Int. Ed. 49 (2010) 676–707.
[2] A.M.R. Smith, K.K. Hii, Chem. Rev. 111 (2011) 1637–1656.
[3] S. Liang, K. Xu, C.C. Zeng, et al., Adv. Synth. Catal. 360 (2018) 4266–4292.
[4] L. Zhu, D. Wang, Z. Jia, et al., ACS Catal. 8 (2018) 5466–5484.
[5] B. List, Acc. Chem. Res. 37 (2004) 548–557.
[6] W. Notz, F. Tanaka, C.F. Barbas, Acc. Chem. Res. 37 (2004) 580–591.
[7] S. Mukherjee, J.W. Yang, S. Hoffmann, et al., Chem. Rev. 107 (2007) 5471–5569.
[8] P. Melchiorre, M. Marigo, A. Carlone, et al., Angew. Chem. Int. Ed. 47 (2008) 6138–6171.
[9] L. Xu, J. Luo, Y. Lu, Chem. Commun. 2009 (2009) 1807–1821.
[10] S. Bertelsen, K.A. Jørgensen, Chem. Soc. Rev. 38 (2009) 2178–2189.
[11] A. Quintard, S. Belot, E. Marchal, et al., Eur. J. Org. Chem. 2010 (2010) 927–936.
[12] M. Nielsen, D. Worgull, T. Zweifel, et al., Chem. Commun. 47 (2011) 632–649.
[13] K.L. Jensen, G. Dickmeiss, H. Jiang, et al., Acc. Chem. Res. 45 (2012) 248–264.
[14] T. Kano, K. Maruoka, Chem. Sci. 4 (2013) 907–915.
[15] B.M. Paz, H. Jiang, K.A. Jorgensen, Chem. Eur. J. 21 (2015) 1846–1853.
[16] S. Meninno, C. Volpe, A. Lattanzi, ChemCatChem 11 (2019) 3716–3729.
[17] T.D. Beeson, A. Mastracchio, J.-B. Hong, et al., Science 316 (2007) 582–585.
[18] M. Mečiarová, P. Tisovský, R. Šebesta, New J. Chem. 40 (2016) 4855–4864.
[19] Y.Q. Zou, F.M. Hörmann, T. Bach, Chem. Soc. Rev. 47 (2018) 278–290.
[20] D. Ma, T.H.F. Wong, P. Melchiorre, Asymmetric photoredox reactions without photocatalysts, in: T. Akiyama, I. Ojima (Eds.), Catalytic Asymmetric Synthesis, 4th ed., John Wiley & Sons, Inc., Hoboken, 2022, pp. 329–354.
[21] D.A. Nicewicz, D.W.C. MacMillan, Science 322 (2008) 77–80.
[22] D.A. Nagib, M.E. Scott, D.W.C. MacMillan, J. Am. Chem. Soc. 131 (2009) 10875–10877.
[23] H.W. Shih, M.N. Vander Wal, R.L. Grange, et al., J. Am. Chem. Soc. 132 (2010) 13600–13603.
[24] M. Neumann, S. Füldner, B. König, et al., Angew. Chem. Int. Ed. 50 (2011) 951–954.
[25] Y. Zhu, L. Zhang, S. Luo, J. Am. Chem. Soc. 136 (2014) 14642–14645.
[26] E. Arceo, I.D. Jurberg, A. Álvarez-Fernández, et al., Nat. Chem. 5 (2013) 750–756.
[27] M. Silvi, E. Arceo, I.D. Jurberg, et al., J. Am. Chem. Soc. 137 (2015) 6120–6123.
[28] A. Bahamonde, P. Melchiorre, J. Am. Chem. Soc. 138 (2016) 8019–8030.
[29] G. Filippini, M. Silvi, P. Melchiorre, Angew. Chem. Int. Ed. 56 (2017) 4447–4451.
[30] E.J. Horn, B.R. Rosen, P.S. Baran, ACS Cent. Sci. 2 (2016) 302–308.
[31] M. Yan, Y. Kawamata, P.S. Baran, Chem. Rev. 117 (2017) 13230–13319.
[32] Y. Jiang, K. Xu, C. Zeng, Chem. Rev. 118 (2018) 4485–4540.
[33] J.-I. Yoshida, A. Shimizu, R. Hayashi, Chem. Rev. 118 (2018) 4702–4730.
[34] T.H. Meyer, I. Choi, C. Tian, et al., Chem 6 (2020) 2484–2496.
[35] C. Zhu, N.W.J. Ang, T.H. Meyer, et al., ACS Cent. Sci. 7 (2021) 415–431.
[36] L.F.T. Novaes, J.J. Liu, Y.F. Shen, et al., Chem. Soc. Rev. 50 (2021) 7941–8002.
[37] X. Cheng, A.W. Lei, T.-S. Mei, et al., CCS Chem. 4 (2022) 1120–1152.
[38] Q.L. Zhang, K. Liang, C. Guo, Sci. China Chem. 67 (2024) 755–758.
[39] W. Zeng, Y. Wang, C. Peng, et al., Chem. Soc. Rev. 54 (2025) 4468–4501.
[40] J. Zhong, Y. Yu, D. Zhang, et al., Chin. Chem. Lett. 32 (2021) 963–972.
[41] W. Zhou, X. Chen, L. Lu, et al., Chin. Chem. Lett. 35 (2024) 08902.
[42] P.Y. Chen, C. Huang, L.H. Jie, et al., J. Am. Chem. Soc. 146 (2024) 7178–7184.
[43] P. Zhou, T. Zou, H.J. Song, et al., Chin. Chem. Lett. 37 (2026) 111673.
[44] S. Rani, N. Sbei, S. Rahali, et al., Chin. Chem. Lett. 36 (2025) 111216.
[45] Q. Lin, L. Li, S. Luo, Chem. Eur. J. 25 (2019) 10033–10044.
[46] M. Ghosh, V.S. Shinde, M. Rueping, Beilstein J. Org. Chem. 15 (2019) 2710–2746.
[47] C. Margarita, H. Lundberg, Catalysts 10 (2020) 982.
[48] X. Chang, Q. Zhang, C. Guo, Angew. Chem. Int. Ed. 59 (2020) 12612–12622.
[49] K.J. Jiao, Z.H. Wang, C. Ma, et al., Chem. Catal. 2 (2022) 3019–3047.
[50] F. Medici, S. Resta, S. Andolina, et al., Catalysts 13 (2023) 944.
[51] J. Rein, S.B. Zacate, K. Mao, et al., Chem. Soc. Rev. 52 (2023) 8106–8125.
[52] C. Gao, X. Liu, M. Wang, et al., Chin. J. Org. Chem. 44 (2024) 673–727.
[53] X. Jiang, C. Zou, W. Zhuang, et al., Green Chem. 27 (2025) 915–945.
[54] Z.-H. Wang, P.-S. Gao, X. Wang, et al., J. Am. Chem. Soc. 143 (2021) 15599–15605.
[55] D. Mazzarella, C. Qi, M. Vanzella, et al., Angew. Chem. Int. Ed. 63 (2024) e202401361.
[56] K.L. Jensen, P.T. Franke, L.T. Nielsen, et al., Angew. Chem. Int. Ed. 49 (2010) 129–133.
[57] N. Fu, L. Li, Q. Yang, et al., Org. Lett. 19 (2017) 2122–2125.
[58] X. Liu, S. Sun, Z. Meng, et al., Org. Lett. 17 (2015) 2396–2399.
[59] X. Liu, Z. Meng, C. Li, et al., Angew. Chem. Int. Ed. 54 (2015) 6012–6015.
[60] G. Zhang, Y. Ma, S. Wang, et al., Chem. Sci. 4 (2013) 2645–2651.
[61] Q. Yang, L. Zhang, C. Ye, et al., Angew. Chem. Int. Ed. 56 (2017) 3694–3698.
[62] H. Hou, S. Zhu, L. Atodiresei, et al., Eur. J. Org. Chem. 2018 (2018) 1277–1280.
[63] F.Y. Lu, Y.J. Chen, Y. Chen, et al., Chem. Commun. 56 (2020) 623–626.
[64] X. Liu, X. Yan, J.H. Yu, et al., Org. Lett. 21 (2019) 5626–5629.
[65] C.L. Dong, X. Ding, L.Q. Huang, et al., Org. Lett. 22 (2020) 1076–1080.
[66] L. Li, Y. Li, N. Fu, et al., Angew. Chem. Int. Ed. 59 (2020) 14347–14351.
[67] R. Francke, R.D. Little, Chem. Soc. Rev. 43 (2014) 2492–2521.
[68] J.E. Nutting, M. Rafiee, S.S. Stahl, Chem. Rev. 118 (2018) 4834–4885.
[69] F. Wang, S.S. Stahl, Acc. Chem. Res. 53 (2020) 561–574.
[70] X. Yang, Z. Xie, Y. Li, et al., Chem. Sci. 11 (2020) 4741–4746.
[71] Y. Chen, Y. Wu, G. Wang, et al., Chin. Chem. Lett. 35 (2024) 109445.
[72] X.H. Ho, S.I. Mho, H. Kang, et al., Eur. J. Org. Chem. 2010 (2010) 4436–4441.
[73] J.Y. He, N.N. Wang, R. Zhao, et al., Eur. J. Org. Chem. 27 (2024) e202400817.
[74] F. Benfatti, M.G. Capdevila, L. Zoli, et al., Chem. Commun. 2009 (2009) 5919–5921.
[75] B. Zhang, S.K. Xiang, L.H. Zhang, et al., Org. Lett. 13 (2011) 5212–5215.
[76] F. Huang, L. Xu, J. Xiao, Chin. J. Chem. 30 (2012) 2721–2725.
[77] E. Larionov, M.M. Mastandrea, M.A. Pericàs, ACS Catal. 7 (2017) 7008–7013.
[78] J.Y. He, C. Zhu, W.X. Duan, et al., Angew. Chem. Int. Ed. 63 (2024) e202401355.
[79] Q. Lin, Y. Duan, Y. Li, et al., Nat. Commun. 15 (2024) 6900.
[80] N.N. Bui, X.H. Ho, S.I. Mho, et al., Eur. J. Org. Chem. 2009 (2009) 5309–5312.
[81] Y. Duan, Y. Zhang, J. Chen, et al., Angew. Chem. Int. Ed. 64 (2025) e202505826.